Article:

eprints@whiterose.ac.uk
https://eprints.whiterose.ac.uk/

Direct-write projection lithography of quantum dot micropillar single photon sources 🔵

Petros Androvitsaneas 🔵 ; Rachel N. Clark 🔵 ; Matthew Jordan 🔵 ; Miguel Alvarez Perez 🔵 ; Tomas Peach 🔵 ;
Stuart Thomas 🔵 ; Saleem Shabbir; Angela D. Sobiesierski 🔵 ; Aristotelis Trapalis 🔵 ; Ian A. Farrer 🔵 ;
Wolfgang W. Langbein 🔵 ; Anthony J. Bennett ✉ 🔵

Check for updates

🌐
View
Online

Export
Citation

CrossMark

Direct-write projection lithography of quantum dot micropillar single photon sources (EP)

Petros Androvitsaneas,[1,2] (iD) Rachel N. Clark,[1,2] (iD) Matthew Jordan,[1,2] (iD) Miguel Alvarez Perez,[1,2] (iD)
Tomas Peach,[3] (iD) Stuart Thomas,[3] (iD) Saleem Shabbir,[3] (iD) Angela D. Sobiesierski,[3] (iD) Aristotelis Trapalis,[4] (iD)
Ian A. Farrer,[4,5] (iD) Wolfgang W. Langbein,[6] (iD) and Anthony J. Bennett[1,2,6,a)] (iD)

AFFILIATIONS

[1] School of Engineering, Cardiff University, Queen's Buildings, The Parade, Cardiff CF24 3AA, United Kingdom
[2] Translational Research Hub, Maindy Road, Cardiff CF24 4HQ, United Kingdom
[3] Institute for Compound Semiconductors, Cardiff University, Queen's Buildings, The Parade, Cardiff CF24 3AA, United Kingdom
[4] Department of Electronic and Electrical Engineering, University of Sheffield, Mappin Street, Sheffield S1 3JD, United Kingdom
[5] EPSRC National Epitaxy Facility, University of Sheffield, Sheffield S3 7HQ, United Kingdom
[6] School of Physics and Astronomy, Cardiff University, Queen's Buildings, The Parade, Cardiff CF24 3AA, United Kingdom

[a)] Author to whom correspondence should be addressed: BennettA19@cardiff.ac.uk

ABSTRACT

We have developed a process to mass-produce quantum dot micropillar cavities using direct-write lithography. This technique allows us to achieve mass patterning of high-aspect ratio pillars with vertical, smooth sidewalls maintaining a high quality factor for diameters below 2.0 μm. Encapsulating the cavities in a thin layer of oxide (Ta_2O_5) prevents oxidation in the atmosphere, preserving the optical properties of the cavity over months of ambient exposure. We confirm that single dots in the cavities can be deterministically excited to create high-purity indistinguishable single photons with interference visibility (0.941 ± 0.008).

Single photon sources are an essential building block for a variety of quantum technologies.[1] Developments in resonant excitation,[2,3] *in situ* lithography,[3,4] and cavity design[5,6] have made quantum dots (QDs) one of the main contenders for high-efficiency and high-indistinguishablity single photon sources. Furthermore, the potential to entangle photons sequentially emitted by the QDs using spin opens up new functionality in entangled photon pair generation,[7–10] cluster state generation,[11] and other higher-dimensional photonic states.[12,13]

One of the most promising cavity designs is the semiconductor micropillar cavity[3,14,15] in which two distributed Bragg reflectors (DBRs) surround a spacer layer containing a low density layer of quantum dots. When etched into circular pillars of approximately 2 μm diameter, these structures confine localized optical modes that enhance photon emission from the QDs, while coupling efficiently to a Gaussian-like mode that can be collected in the far field. A key challenge is achieving a deep vertical etch; this requires balancing the chemical and mechanical properties of the etch to manage the rate of re-deposition and minimize damage to the mask layer. Furthermore, the etched pillar sides must be smooth to limit the scattering loss and

maintain a high quality factor (Q) and light collection efficiency. Therefore, fabrication requires a hard mask that is able to withstand the aggressive etch needed to remove up to 10 μm of the semiconductor, but which is thin enough to be patterned with the necessary high accuracy. Different approaches to masking for this purpose have been demonstrated, including randomly positioned sapphire nanocrystals,[16] contact lithography with a quartz mask,[17] electron beam lithography,[18] and cryogenic *in situ* laser-lithography.[4] The latter two allow for pre-selection of promising QDs and alignment of cavities but are expensive and less compatible with mass production of devices.

Here, we report a direct-write photolithography method allowing high-throughput sample patterning for deep etches of GaAs. This technique, also known as mask-less lithography, uses a UV light source and a digital light modulator to project the pattern onto the sample with potential to reconfigure designs by software. It provides the flexibility of electron beam lithography, at a lower cost, and with a 400 nm resolution that is sufficient for this application. Characterization of the cavities shows they have low sidewall scattering parameters, retaining high Q-factors even at low diameters. Finally, we

demonstrate a high brightness, high purity, and indistinguishable single photon source using deterministic pulsed resonant excitation to verify the quality of the material.

The samples were grown by molecular beam epitaxy with ∼0.5% variation in growth rate over the 3-in. wafer, resulting in a uniform dot density. A high Q cavity sample was grown consisting of a lower Bragg mirror of 26 pairs of alternating $Al_{0.95}Ga_{0.05}As$[19] and GaAs $\lambda/4$ layers, a single wavelength spacer with InAs QDs at its center, and a final 17 pair Bragg mirror. A low Q cavity was also grown with 7/26 Bragg mirror pairs, both with a design wavelength of 940 nm. The processing proceeds as shown in Fig. 1(a) by coating the chips with a hard-mask layer of 750 nm SiO_2 deposited via plasma enhanced chemical vapor deposition (PECVD). A 2 μm layer of negative photoresist, AZ2020, is applied and exposed using the MicroWriter ML3 Pro direct-write photo-lithography tool. The pattern consists of disks with diameters in the range of 1.55–5.00 μm in regularly spaced 5×5 arrays. This direct-write method allows for the patterning of 14 000 devices in 240 s, which we estimate is two orders of magnitude faster than electron beam lithography. After developing the photoresist in AZ726, the hard mask is etched using a C_4F_8/O_2 inductively coupled plasma (ICP) and the photo-resist removed. The semiconductor is then etched using a $Cl_2/BCl_3/N_2$ ICP, and the hard mask is then removed with a second C_4F_8/O_2 etch. Finally, the micropillars are encapsulated in a 10 nm layer of Ta_2O_5 using atomic layer deposition.
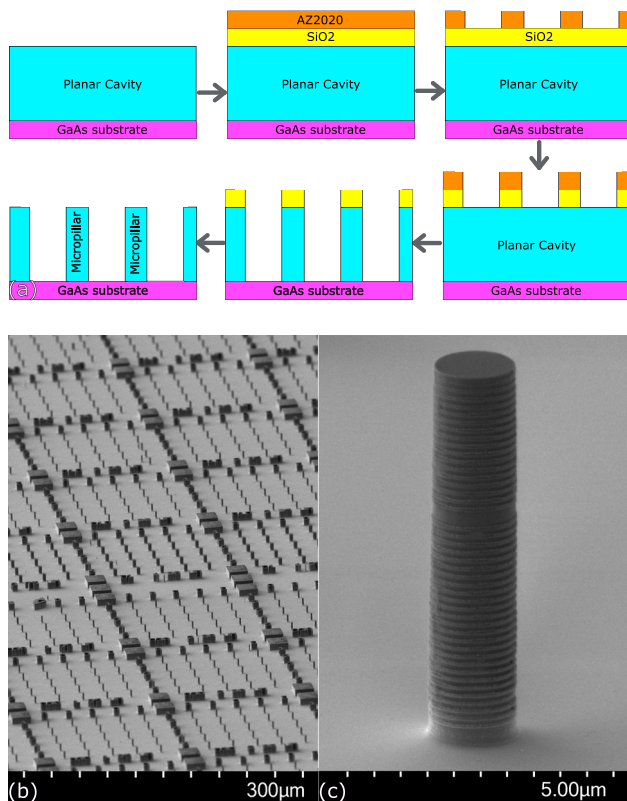
This oxide layer provides a uniform conformal coating that protects the samples against oxidation, especially for the DBR layers containing aluminum.[5] Between 1 and 2 cavities out of 200 micropillars with diameters below 2 μm are critically damaged and display no emission at all, not even off-resonant feeding of the cavity mode. Among the remaining majority, which show some emission, the overall yield of micropillars with sharp QD emission lines within the FWHM of the cavity mode is 0.5% for a high Q-factor sample. All cavities in the low Q sample have such lines within the mode, as a result of the rather high areal density of dots.

The quality of the patterning and semiconductor etch determines the sidewall roughness, which introduces losses to the cavity mode HE_{11}.[18] The overall loss rate for photons in the mode is inversely proportional to the quality factor at a given diameter, $1/Q(d) = 1/Q_0 + 1/Q_s(d)$, where the decay rate due to sidewall roughness is parameterized by $1/Q_s(d)$, which adds to the loss rate through mirrors $1/Q_0$. Q_0 can be determined from the Q-factor that cavities tend toward at high diameter. $Q_s(d)$ is linked to the diameter of the micropillar by the following expression $1/Q_s(d) = 2k_s J_0^2(kd/2)/d$, where k_s is the sidewall loss coefficient and $J_0(kd/2)$ is the zeroth order Bessel function with k being the transverse wavevector and d the diameter.[18]

The high Q-factor structure allows us to measure any losses resulting from sidewall roughness created during the lithography and etch processes. Two different techniques have been utilized to measure the cavity's $Q(d)$, photoluminescence (PL) and white light reflectivity (WLR), with example data shown in Figs. 2(a) and 2(b). The relatively high density of spectrally sharp QD transitions in the spectral range of the mode made the measurement of Q using PL at 4 K unreliable. Therefore, the WLR measurement was used to determine the Q-factor of HE_{11} at this temperature, Fig. 2(c). Additionally, we measure the Q-factors at 80 K using PL [Fig. 2(d)] and WLR [Fig. 2(e)]. All three data-sets yield a similar value for the sidewall loss coefficient k_s, (c) k_s of (48 ± 9) pm, (d) (50 ± 20) pm, and (e) (60 ± 20) pm. These values are comparable to the state-of-the-art for these photonic structures[18] which reports $k_s = 68$ pm. The Q-factor of the 1.85 μm cavity is approximately one third of the value estimated in our simulations,
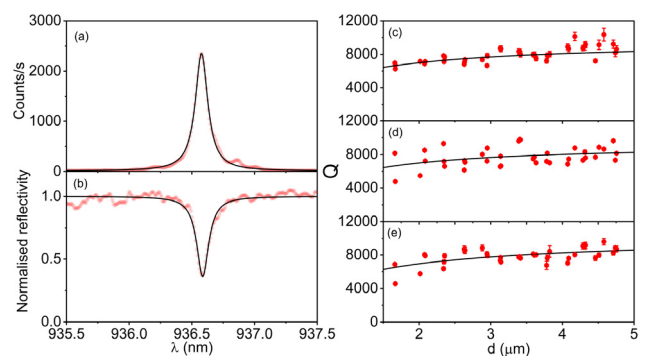

FIG. 1. Micropillar fabrication. (a) Schematic of processing steps. (b) Wide area scanning electron microscope image (SEM) of etched structures with a variety of different diameters. (c) SEM of a high Q-factor micropillar of diameter 1.75 μm.

FIG. 2. Cavity quality factors. (a) Photoluminescence (PL) spectrum of the cavity mode (red data points) with the corresponding Lorentzian fit (black line) of a micropillar consisting of 17/26 period Bragg mirrors and a diameter $d = 3.14$ μm at 80 K, yielding a $Q = 7740 \pm 60$. (b) Normalized white light reflectivity (WLR) (red data points) for the same micropillar at 80 K with the Lorentzian fit (black line), yielding a $Q = 8100 \pm 300$. (c) $Q(d)$ measured at 4 K by WLR. (d) $Q(d)$ measured at 80 K by PL and (e) by WLR. Fits shown as black lines discussed in the text.

suggesting the maximum Purcell Factor that could be observed would be similarly reduced to a value of 25.

In the course of our studies, we have confirmed dots in both cavity designs display antibunching to a few % level under weak resonant CW excitation, as expected.[17,20] Several previous reports have shown highly indistinguishable (>0.9 visibility) quantum light emission under pulsed resonant excitation in pillar cavities of comparable high Q, where the reduction in radiative lifetime is expected to improve the indistinguishability.[3,6,14] More surprisingly, we find that the quality of the dots in this material is sufficient to generate highly indistinguishable photons under resonant excitation with only a modest Purcell factor of ~3 in a low Q sample. The sample was stored in air for three months after the processing with no observable degradation in Q or emission. It has been shown that these low Q cavities can be efficient and broadband.[21,22] A standard dark field microscope setup is used[20] in which the input can be swapped between laser excitation and a broadband light emitting diode for reflectivity. The cross-polarized resonantly scattered light is collected into a polarization maintaining fiber and directed to a spectrometer or superconducting nanowire single photon detectors (SNSPDs). Optical losses, polarization filtering, and SNSPD detector efficiency combine to give an overall system efficiency of $(4.5 \pm 0.6)\%$.

We study a neutral exciton on resonance with the HE_{11} in a 1.7 μm diameter micropillar with a low Q-factor ($Q = 440 \pm 30$) and 7/26 Bragg mirror pairs. This exciton displays a fine structure splitting of 11 μeV, and the corresponding beat is observed within the radiative decay time of 480 ps. Finite-difference time-domain (FDTD) simulations performed using Ansys Lumerical[23] using a horizontal electric dipole at the center of the cavity, driven as a pulse of 5.6 ps duration over a spectral range from 845 to 1060 nm and at the frequency of the HE_{11} mode, reveal a maximum Purcell factor of 3.16 with an overall expected efficiency of up to 0.79 at the collection objective above the pillar. Measurements of a control sample with similar dots and no cavity reveal a mean radiative lifetime of 1.30 ns, which indicates the transition reported here has a Purcell factor of 2.70.

Exciting the transition resonantly in a cross-polarized geometry,[20] we vary the pulse amplitude to observe a Rabi oscillation. With π-pulse excitation, the maximum count-rate is ~2.2 MHz, measured by an SNSPD, see Fig. 3(a), which corresponds to a "first lens brightness" of 64%. A second order autocorrelation measurement reveals the purity of the single photon emission,[24] when the system undergoes a full population inversion under the excitation of the π-pulse to give $g^{(2)}(0) = 0.027 \pm 0.004$, see Fig. 3(b).

Finally, we measure the indistinguishability of the single photons emitted under the conditions described above by interfering two sequentially emitted photons from the QD, Fig. 3(c). This yields a raw visibility of the two-photon interference 0.889 ± 0.006, Figs. 3(d) and 3(e). We infer the indistinguishability value by accounting for the finite
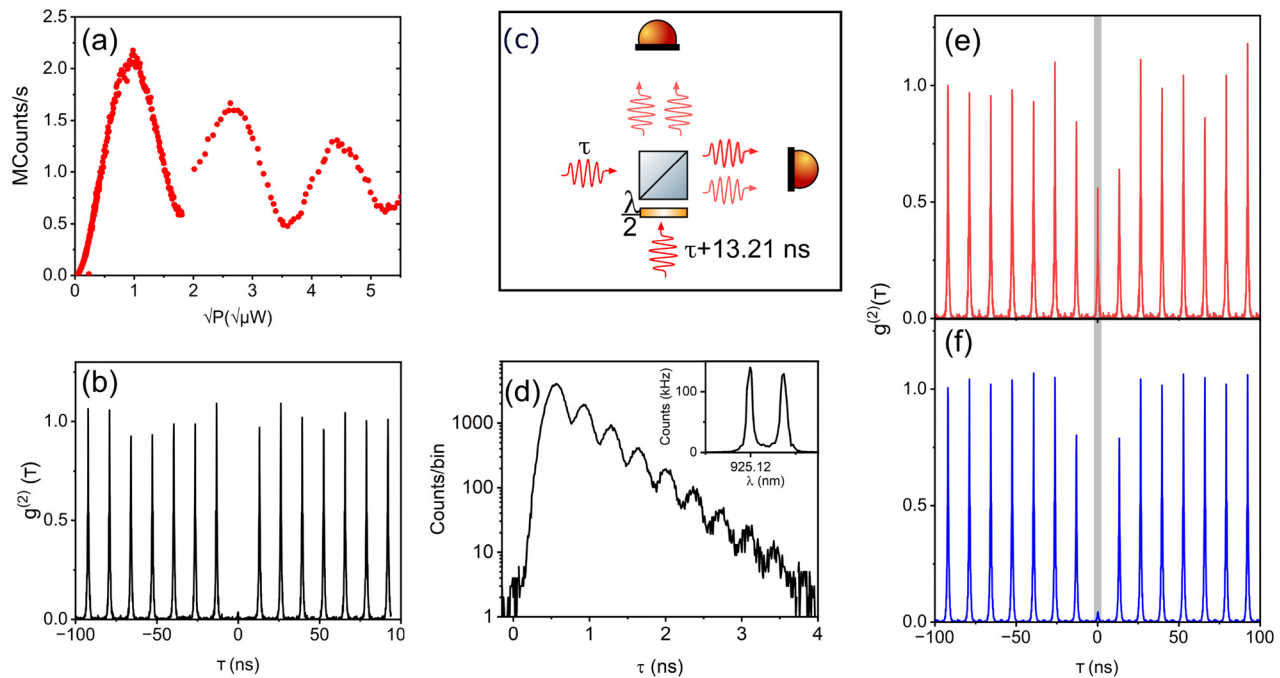
FIG. 3. Indistinguishable single photons from a deterministically driven neutral exciton transition in a micropillar. (a) Rabi oscillation in the pulse amplitude for a neutral exciton in a 7/26 period Bragg mirror cavity, the discontinuity at the point of 2π stems from the measurement using a neutral density filter to allow the two power ranges. (b) Pulsed $g^{(2)}(\tau)$ produced by fully inverting the system using a π-pulse, at a power of 0.969 $\sqrt{\mu W}$, with $g^{(2)}(0) = 0.027 \pm 0.004$. (c) Setup used to interfere two subsequent photons generated 13.2 ns apart. A half waveplate ($\lambda/2$) is used to introduce polarization indistinguishability. The interferometer used had a first order visibility of 0.950 ± 0.002, characterized with a narrow (<1 MHz) single frequency laser at the same approximate wavelength. (d) Time resolved emission intensity after a short pulse showing a beat which arises from the exciton's fine structure splitting (shown in the CW laser resonance fluorescence spectral scan, inset). (e) Hong–Ou–Mandel (HOM) interference measurement for orthogonally polarized photons and (f) co-polarized photons. The visibility is 0.889 ± 0.006, derived by the ratio of the areas denoted by the shaded rectangle. Correlations are normalized by the mean area at large delays. Accounting only for multi-photon emission from the source, $g^{(2)}(0)$, the inferred indistinguishability is 0.941 ± 0.008.

TABLE I. Performance metrics of five sources in the sample.

λ (nm)	Rate (MHz)[a]	$g^{(2)}(0)$	HOM visibility[b]	Lifetime (ps)
925.12[c]	2.2	0.027	0.941	480
925.35	2.1	0.021	0.920	474
924.62	1.6	0.028	0.907	449
925.35	0.9	0.044	0.916	471
925.91	1.5	0.066	0.932	545

[a]Under π-pulse excitation.
[b]Recorded under π-pulse excitation and corrected for finite $g^{(2)}(0)$.
[c]This is the dot discussed in Fig. 3.

$g^{(2)}(0)$ to be 0.941 ± 0.008.[25] This value is comparable to the visibility achieved with QDs in cavities with higher Purcell factors.[1,3,5,14,15] This shows the excellent condition of the material even after the prolonged exposure to a non-controlled atmosphere. In the course of preparing this manuscript, we measured similar results on a number of dots, which is summarized in Table I. This shows the reproducibility of the results in cavities on the same chip, albeit with the inherent bias of pre-selecting transitions that are spectrally isolated and bright under non-resonant excitation.

This direct-write method can be used for high-volume manufacturing of QD micropillar devices. The quality of the structure, low sidewall roughness, and high-purity of the indistinguishable photons show its promise as a flexible platform for mass production of single photon sources. Future work could improve the collection efficiency into a single mode fiber by optimizing the far field emission pattern. An increased yield of optimized structures could be achieved by mapping the locations of dots prior to the processing, facilitating the repositioning of cavities and dots over a whole chip without the need for cryogenic lithography.[4] Furthermore, with positioned arrays of QDs becoming available,[26] the yield could approach unity.

AUTHOR DECLARATIONS
Conflict of Interest

The authors have no conflicts to disclose.

Author Contributions

Petros Androvitsaneas: Conceptualization (lead); Data curation (lead); Formal analysis (lead); Investigation (lead); Methodology (lead); Writing – original draft (lead); Writing – review & editing (equal). **Ian Farrer:** Conceptualization (equal); Investigation (equal); Methodology (equal). **Wolfgang Werner Langbein:** Investigation (equal); Methodology (equal); Supervision (equal). **Anthony J. Bennett:** Conceptualization (equal); Data curation (equal); Formal analysis (equal); Funding acquisition (lead); Investigation (equal); Methodology (equal); Project administration (lead); Resources (lead); Supervision (lead); Writing – review & editing (equal). **Rachel N. Clark:** Investigation (equal); Methodology (equal); Writing – review & editing (equal). **Matthew Jordan:** Formal analysis (equal); Investigation (equal); Writing – review & editing (equal). **Miguel Alvarez Perez:** Investigation (supporting). **Tomas Peach:** Conceptualization (equal); Investigation (equal); Methodology (equal); Writing – review & editing (equal). **Stuart Thomas:** Conceptualization (equal); Investigation (equal); Methodology (equal). **Saleem Shabbir:** Investigation (equal); Methodology (equal). **Angela Sobiesierski:** Conceptualization (equal); Investigation (equal); Methodology (equal); Writing – review & editing (equal). **Aristotelis Trapalis:** Conceptualization (equal); Investigation (equal); Methodology (equal).

DATA AVAILABILITY

The data that support the findings of this study are openly available in the Cardiff University Research Portal at https://doi.org/10.17035/d.2023.0257041928, Ref. 27.

REFERENCES

[1]Y. Arakawa and M. J. Holmes, Appl. Phys. Rev. **7**, 021309 (2020).

[2]E. B. Flagg, A. Muller, J. Robertson, S. Founta, D. Deppe, M. Xiao, W. Ma, G. Salamo, and C.-K. Shih, Nat. Phys. **5**, 203 (2009).

[3]N. Somaschi, V. Giesz, L. De Santis, J. Loredo, M. P. Almeida, G. Hornecker, S. L. Portalupi, T. Grange, C. Anton, J. Demory et al., Nat. Photonics **10**, 340 (2016).

[4]A. Dousse, L. Lanco, J. Suffczyński, E. Semenova, A. Miard, A. Lemaître, I. Sagnes, C. Roblin, J. Bloch, and P. Senellart, Phys. Rev. Lett. **101**, 267404 (2008).

[5]N. Tomm, A. Javadi, N. O. Antoniadis, D. Najer, M. C. Löbl, A. R. Korsch, R. Schott, S. R. Valentin, A. D. Wieck, A. Ludwig et al., Nat. Nanotechnol. **16**, 399 (2021).

[6]Y.-M. He, Y. He, Y.-J. Wei, D. Wu, M. Atatüre, C. Schneider, S. Höfling, M. Kamp, C.-Y. Lu, and J.-W. Pan, Nat. Nanotechnol. **8**, 213 (2013).

[7]R. M. Stevenson, R. J. Young, P. Atkinson, K. Cooper, D. A. Ritchie, and A. J. Shields, Nature **439**, 179 (2006).

[8]R. J. Young, R. M. Stevenson, P. Atkinson, K. Cooper, D. A. Ritchie, and A. J. Shields, New J. Phys. **8**, 29 (2006).

[9]A. Dousse, J. Suffczyński, A. Beveratos, O. Krebs, A. Lemaître, I. Sagnes, J. Bloch, P. Voisin, and P. Senellart, Nature **466**, 217 (2010).

[10]F. B. Basset, M. B. Rota, C. Schimpf, D. Tedeschi, K. D. Zeuner, S. C. Da Silva, M. Reindl, V. Zwiller, K. D. Jöns, A. Rastelli, and R. Trotta, Phys. Rev. Lett. **123**, 160501 (2019).

[11]I. Schwartz, D. Cogan, E. R. Schmidgall, Y. Don, L. Gantz, O. Kenneth, N. H. Lindner, and D. Gershoni, Science **354**, 434 (2016).

[12]J. P. Lee, B. Villa, A. J. Bennett, R. M. Stevenson, D. J. P. Ellis, I. Farrer, D. A. Ritchie, and A. J. Shields, Quantum Sci. Technol. **4**, 025011 (2019).

[13]M. H. Appel, A. Tiranov, S. Pabst, M. L. Chan, C. Starup, Y. Wang, L. Midolo, K. Tiurev, S. Scholz, A. D. Wieck et al., Phys. Rev. Lett. **128**, 233602 (2022).

[14]X. Ding, Y. He, Z. C. Duan, N. Gregersen, M. C. Chen, S. Unsleber, S. Maier, C. Schneider, M. Kamp, S. Höfling, C.-Y. Lu, and J.-W. Pan, Phys. Rev. Lett. **116**, 020401 (2016).

[15]H. Wang, Y.-M. He, T.-H. Chung, H. Hu, Y. Yu, S. Chen, X. Ding, M.-C. Chen, J. Qin, X. Yang, R.-Z. Liu, Z.-C. Duan, J.-P. Li, S. Gerhardt, K. Winkler, J. Jurkat, L.-J. Wang, N. Gregersen, Y.-H. Huo, Q. Dai, S. Yu, S. Höfling, C.-Y. Lu, and J.-W. Pan, Nat. Photonics **13**, 770 (2019).

[16]C. Santori, D. Fattal, J. Vučković, G. S. Solomon, and Y. Yamamoto, Nature **419**, 594 (2002).

[17] A. J. Bennett, J. P. Lee, D. J. P. Ellis, I. Farrer, D. A. Ritchie, and A. J. Shields, Nat. Nanotechnol. **11**, 857 (2016).

[18] C. Schneider, P. Gold, S. Reitzenstein, S. Höfling, and M. Kamp, Appl. Phys. B **122**, 19 (2016).

[19] N. Cho, K. Kim, J. Song, W. Choi, and J. Lee, Solid State Commun. **150**, 1955 (2010).

[20] A. V. Kuhlmann, J. Houel, D. Brunner, A. Ludwig, D. Reuter, A. D. Wieck, and R. J. Warburton, Rev. Sci. Instrum. **84**, 073905 (2013).

[21] P. Androvitsaneas, A. B. Young, C. Schneider, S. Maier, M. Kamp, S. Höfling, S. Knauer, E. Harbord, C. Y. Hu, J. G. Rarity, and R. Oulton, Phys. Rev. B **93**, 241409 (2016).

[22] L. Ginés, M. Moczała-Dusanowska, D. Dlaka, R. Hošák, J. R. Gonzales-Ureta, J. Lee, M. Ježek, E. Harbord, R. Oulton, S. Höfling *et al.*, Phys. Rev. Lett. **129**, 033601 (2022).

[23] Ansys Lumerical, see https://optics.ansys.com/hc/en-us/articles/360041612594-Purcell-factor-of-a-microdisk for "Purcell factor of a microdisk" (2023).

[24] R. H. Brown and R. Q. Twiss, London, Edinburgh, Dublin Philos. Mag. J. Sci. **45**, 663 (1954).

[25] H. Ollivier, S. Thomas, S. Wein, I. M. de Buy Wenniger, N. Coste, J. Loredo, N. Somaschi, A. Harouri, A. Lemaitre, I. Sagnes *et al.*, Phys. Rev. Lett. **126**, 063602 (2021).

[26] J. Große, M. von Helversen, A. Koulas-Simos, M. Hermann, and S. Reitzenstein, APL Photonics **5**, 096107 (2020).

[27] P. Androvitsaneas, R. Clark Rachel, M. Jordan, M. Alvarez Perez, T. Peach, S. Shabbir, A. Sobiesierski, A. Trapalis, I. Farrer, W. Langbein, and A. J. Bennett (2023). "Direct-write projection lithography of quantum dot micropillar single photon sources: Data," Cardiff University Research Portal. https://doi.org/10.17035/d.2023.0257041928

27 November 2023 15:29:47